



This is a repository copy of *Optimal decision-making in mammals : insights from a robot study of rodent texture discrimination*.

White Rose Research Online URL for this paper:
<http://eprints.whiterose.ac.uk/155165/>

Version: Accepted Version

Article:

Lepora, N.F., Fox, C.W., Evans, M.H. et al. (3 more authors) (2012) Optimal decision-making in mammals : insights from a robot study of rodent texture discrimination. *Interface*, 9 (72). pp. 1517-1528. ISSN 1742-5689

<https://doi.org/10.1098/rsif.2011.0750>

© 2012 The Royal Society. This is an author-produced version of a paper subsequently published in *Interface*. Uploaded in accordance with the publisher's self-archiving policy.

Reuse

Items deposited in White Rose Research Online are protected by copyright, with all rights reserved unless indicated otherwise. They may be downloaded and/or printed for private study, or other acts as permitted by national copyright laws. The publisher or other rights holders may allow further reproduction and re-use of the full text version. This is indicated by the licence information on the White Rose Research Online record for the item.

Takedown

If you consider content in White Rose Research Online to be in breach of UK law, please notify us by emailing eprints@whiterose.ac.uk including the URL of the record and the reason for the withdrawal request.



eprints@whiterose.ac.uk
<https://eprints.whiterose.ac.uk/>

Optimal decision making in mammals:
Insights from a robot study of rodent texture discrimination

Nathan F. Lepora¹, Charles W. Fox¹, Mathew H. Evans¹,
Mathew E. Diamond², Kevin Gurney¹ and Tony J. Prescott¹

¹ *Department of Psychology, University of Sheffield, Sheffield, UK, S10 2TP.*

² *International School for Advanced Studies (SISSA), Trieste, Italy.*

Running head: Robot texture discrimination

Key words: Biomimetics, perception, decision making,
Bayes rule, whiskers, texture.

December 29, 2011

Abstract

Texture perception is studied here in a physical model of the rat whisker system consisting of a robot equipped with a biomimetic vibrissal sensor. Investigations of whisker motion in rodents have led to several explanations for texture discrimination, such as resonance or stick-slips. Meanwhile, electrophysiological studies of decision making in monkeys have suggested a neural mechanism of evidence accumulation to threshold for competing percepts, described by a probabilistic model of Bayesian sequential analysis. For our robot whisker data, we find that variable reaction-time decision making with sequential analysis performs better than fixed response-time maximum likelihood estimation. These probabilistic classifiers also utilize whatever available features of the whisker signals aid the discrimination, giving improved performance over a single-feature strategies such as matching the peak power spectra of whisker vibrations. These results cast new light on how the various proposals for texture discrimination in rodents depend on the whisker contact mechanics and suggest the possibility of a common account of decision making across mammalian species.

1 Introduction

The last fifteen years has seen major advancement in the understanding of human and animal perception as statistically optimal inference from noisy and ambiguous sensations. This statistical approach is based on using Bayes' rule to calculate the conditional probability distribution over possible percepts given sensory data, knowing aspects of the world such as the likelihood of sensory data for various percepts and their prior probabilities of occurring [1, 2]. In neuroscience there has been parallel progress in understanding perceptual decision making as evidence accumulation for competing hypotheses. One notable line of experiments considers neuronal activity in parietal cortex as monkeys make perceptual judgements about the direction of motion for a group of random dots, and finds individual neurons that noisily ramp-up their firing rates until reaching a threshold when a decision is made [3, 4]. Theoretically, these processes appear well described by the statistical approach of sequential analysis [5, 6], which applies Bayes' rule to accumulate evidence for competing perceptual hypotheses over time series of sensory data until reaching a preset threshold [7].

This article aims to help develop a paradigm in rodents for testing this Bayesian approach to perceptual decision making from the dual perspectives of guiding biological experimentation and testing biological hypotheses in robots with biomimetic sensors. Our particular focus is on texture discrimination using vibrissae, which is both a well-developed approach for examining decision making in rats [8, 9, 10, 11, 12, 13, 14, 15, 16] and a task for which state-of-the-art sensors based on rat whiskers are under continued development [17, 18, 19, 20, 21, 22, 23, 24]. Furthermore, in biological systems there are several proposals for which features of whisker motion vary according to texture, for example the resonance hypothesis [16] and the kinetic signature hypothesis [15]. However, it is not known how these proposals relate to theories of perceptual decision making via evidence accumulation and how they would function in practice when embodied in a biologically inspired robot.

Our overall hypothesis is that Bayesian sequential analysis can also account for texture discrimination in rats, and thus offer a common account of decision making in different mammalian species. The first part of this hypothesis is that the brain makes perceptual decisions by applying Bayesian inference to time series of sensory data over the motion of the whisker contacts, by comparing posterior probabilities (or functions thereof) with predefined thresholds. The second part of this hypothesis is that the brain utilizes simplifying assumptions about the sensory data to reduce the complexity of the neural computation. In particular, the principal assumption underlying sequential analysis is that the data samples are independently distributed over time and drawn randomly from sampling

distributions associated with the likelihood functions. In computational neuroscience, it is commonly assumed that these sampling distributions are Gaussian [5], but we find that this assumption is too restrictive for a whiskered robot sensing texture. Instead, we assume that both the robot and animal are able to encode more general probability distributions of sensed data.

These proposals for rodent decision making are investigated in a physical model of the rat whisker system consisting of a robot equipped with a biomimetic vibrissa sensor. Our particular platform is a Roomba robot (iRobot, Boston MA) with attached whisker module (Fig. 1), an ideal device for performing whisker-based experiments on surface texture because the robot can either move autonomously or be guided [25]. This investigation reveals how biomimetic principles can guide the development of new technologies and in turn provide a greater understanding of the biological systems. In particular, we conclude that decision making with variable reaction times based on Bayesian sequential analysis out-competes existing alternative methods, including both non-Bayesian and maximum likelihood (fixed-response time) classifiers. A second observation is that probabilistic perception utilizes whatever aspects of the contact dynamics help discriminate the alternatives, so that the various proposals for how whisker motion varies according to texture could all give reliable classification depending upon the contact mechanics of the whisker and surface.

Some partial results have been published in two conference papers, on feature-based classifiers [25] and a preliminary version of the probabilistic analysis [26] based on a similar method to the maximum likelihood classifier discussed here (but referred to as ‘naive’ Bayes).

Figure 1 about here (1.5 column)

2 Texture sensing with biomimetic whiskers

Touch sensors inspired by mammalian vibrissae have been in development since the 1980s (see [17]). Recently, biomimetic whisker sensors have been engineered to have shape and material properties similar to those of rat whiskers, while scaled to larger sizes appropriate for autonomous robots [21, 27]. Another recent innovation is that the whisker deflections are transduced into sensory signals with a miniature Hall-effect sensor mounted at the base of the artificial whisker shaft [28]. Arrays of these whiskers have been employed in robots based on the rat whisker system [27, 28] and could serve a variety of functions on mobile robots [17, 19, 22].

The biomimetic whisker was mounted on the front of the Roomba robot (Fig. 1) at 45 degree azimuth from the forwards direction of travel with a slight downwards elevation sufficient to make constant contact with the floor during movement. Outputs from the whisker sensor included two voltages, x and y , with magnitudes linearly proportional to the tangential component of the two orthogonal displacement angles of the magnet from its resting position (with the x -component parallel to the contact surface and the y -component normal to it). As the robot moved, the whiskers were swept across the floor. The deflections of the whisker were acquired at a rate of 2 kHz and sent to a computer through the BRAHMS execution framework [29] for analysis in MATLAB (Mathworks, Natick MA).

Four surfaces were chosen for classification: two carpets of different roughnesses, a tarmac surface and a vinyl surface (Fig. 1). These surfaces were chosen because they were appropriately generic for a real world experiment and they provided a range of surface types that were sufficiently similar to make classification non-trivial. Two primary behavioral conditions were also chosen: where the robot moved in a stereotyped manner, rotating either anticlockwise only, or clockwise only (four trials of each motion of sixteen seconds each) and where the robot moved autonomously using its motion guidance, consisting of externally unpredictable clockwise, anticlockwise and forward motions (four trials of sixteen seconds¹). Data from the four floor surfaces are shown in Fig. 2 for the stereotyped motion and Fig. 3 for the autonomous motion.

Figures 2 and 3 about here (double column, on single page)

¹Trials 13-16 of ref. [25]. Trials 9-12 were rejected because of a systematic change in whisker baseline position during trial 12, due to the whisker module becoming detached from the robot (see also [26, Fig. 6]).

3 Probabilistic classification and decision making

To introduce the relation between decision making in neuroscience and inference over sequentially sampled sensory data, we recall work by Gold and Shadlen on the decision making of two alternative forced choices [5, 30]. They argued that electrophysiological recordings from LIP association cortex in awake behaving monkeys [4] match well with hypothesis testing by the sequential probability ratio test. The log likelihood ratio log LR is central to this interpretation because it indicates whether alternative H_1 or H_2 is supported by a sample of sensory data s , as follows from using Bayes rule $p(H_k|s) = p(s|H_k)p(H_k)/p(s)$ to derive

$$\begin{aligned} \log \text{PR}(s) &= \log \text{LR}(s) + \log \text{HR}, \\ \log \text{PR}(s) &= \log \frac{p(H_1|s)}{p(H_2|s)}, \quad \log \text{LR}(s) = \log \frac{p(s|H_1)}{p(s|H_2)}, \quad \log \text{HR} = \log \frac{p(H_1)}{p(H_2)}, \end{aligned} \tag{1}$$

where log PR is the log posterior ratio and log HR is the log prior ratio. For a known likelihood ratio function of the sampling distributions, the decision of whether hypothesis H_k is supported to a given (log) reliability Θ_k is determined by threshold-crossing, such that if $\log \text{PR}(s) \geq \Theta_k$ then H_k is supported (corresponding to upwards and downwards threshold crossing, as depicted in [5, Fig. 2b]). Considering many such independent identically-distributed samples, the log likelihood ratio becomes a sum of individual terms with the threshold-crossing rule determining when there is sufficient evidence to make a decision

$$\log \text{LR}(s_1, \dots, s_n) = \sum_{i=1}^n \log \text{LR}(s_i) \geq \Theta_k - \log \text{HR}. \tag{2}$$

The similarity of this decision process to the observed accumulation of neural activity to threshold provides strong motivation that the relation between the log likelihood ratio and log posterior ratio gives a natural way of ‘trading off sensory information, prior probability and expected value to form a perceptual decision’ [30]. In particular, decision making with the sequential probability ratio test optimizes the cost of making errors plus the cost per sample time of delaying the decision [7]. Thus for a given accuracy, it gives the fastest reaction time (see [5, 6]).

How should this Bayesian approach to decision making be applied to multiple competing alternatives? Denoting the training data from the four choices as T_1, \dots, T_4 (for rough carpet, smooth carpet, tarmac and vinyl flooring, respectively), the sampling distributions for single samples s are

$$P(s|T_k) \equiv P(q(s)|T_k) = \frac{n_q(T_k)}{\sum_{q=1}^N n_q(T_k)}, \tag{3}$$

where $n_q(\mathbb{T}_k)$ is the total number of times that the binned sample value $q(s)$ occurs over the time series and N is the number of bins. We consider pairs $s = (x, y)$ of sampled voltage data corresponding to the two-dimensional whisker deflections, which for simplicity are assumed independent so that $P(x, y|\mathbb{T}_k) = P(x|\mathbb{T}_k)P(y|\mathbb{T}_k)$. The likelihoods associated with these sampling distributions can then be used to define a probabilistic classifier to discriminate the four choices of textures.

Given some test data to be classified, the log posterior probability that its samples are drawn from the training data for choice \mathbb{T}_k is found from the logarithm of Bayes rule

$$\log P(\mathbb{T}_k|s_1, \dots, s_n) = \log P(s_1, \dots, s_n|\mathbb{T}_k) + \log P(\mathbb{T}_k) - \log P(s_1, \dots, s_n), \quad (4)$$

where $P(\mathbb{T}_k)$ is the prior probability of the data being from texture \mathbb{T}_k . Here $\log P(s_1, \dots, s_n)$ is a normalization term that ensures the posteriors sum to unity, and is found by summing the likelihoods and priors over all textures

$$\log P(s_1, \dots, s_n) = \log \left[\sum_{k=1}^4 P(s_1, \dots, s_n|\mathbb{T}_k) P(\mathbb{T}_k) \right]. \quad (5)$$

Considering conditionally independent and identically distributed samples for each choice of texture, an estimator for the log likelihood is a sum of individual terms with

$$\log P(s_1, \dots, s_n|\mathbb{T}_k) = \frac{1}{m} \sum_{i=1}^n \log P(s_i|\mathbb{T}_k), \quad (6)$$

where $m > 0$ is a normalization (see below). The log posteriors are then found by evaluating Eqs 4-6 over n samples of training data.

Note that in practice we evaluated the log posteriors from the estimated log likelihoods in discrete steps (here every 20 samples, or 10 ms). Mathematically, the likelihood to the right of Eq. 6 should be normalized by the number of combinations that could give the particular histogram of measurement values $\{n_q\}$ in Eq. 3, otherwise the small values of the estimated likelihoods could present numerical floating point issues when calculating the posteriors (Eq. 5). All log likelihoods were thus accumulated with a normalization factor $m = 20$ in Eq. 6, equivalent to using the average log likelihood as an estimator [31].

This study compares and contrasts two types of probabilistic classifier based on the accumulated log likelihoods (6). Both classifiers assume there is no biasing from prior knowledge of the occurrence frequency of the textures, so that the prior probabilities $P(\mathbb{T}_k) = 1/4$ are equal.

(i) Maximum likelihood classifier: The first probabilistic classifier considers the number of samples n as a constant set in advance of the decision making. Then the most probable choice of

texture T_k to have produced the test data has the largest log posterior probability, corresponding to the maximal *a posteriori* estimate

$$T = \arg \max_{T_k} P(T_k | s_1, \dots, s_n) = \arg \max_{T_k} \left[\sum_{i=1}^n \log P(s_i | T_k) \right], \quad (7)$$

where we have used that both the normalizing term and prior are texture independent and can be ignored in the arg max operation. The probabilistic classification is then maximum likelihood estimation over a fixed window of test data.

(ii) Sequential Bayes classifier: By analogy with the sequential probability ratio test, the decision of when a choice of texture is supported to a given log reliability θ_k is determined by when a log posterior crosses its threshold

$$\log P(T_k | s_1, \dots, s_n) > \theta_k, \quad (8)$$

which determines the number of samples n used for the classification. We then take the most probable choice of texture T to have generated the test data as the above maximal *a posteriori* estimate (Eq. 7).

For two choices, Bayesian sequential analysis (Eq. 8) is formally equivalent to the sequential probability ratio test (Eq. 2) with $\Theta_k = \theta_k / (1 - \theta_k)$, as follows by rearranging the threshold conditions. For given thresholds, it thus gives the fastest decision times [7]. For more than two choices, there exist more complicated sequential probability ratio methods that are asymptotically optimal [32], in that they give the fastest decisions as the number of samples approaches infinity. In this study, we are concerned with decision making over finite sample numbers on data that may invalidate optimality assumptions such as sample independence. Therefore, for simplicity, we confine our treatment to the fixed duration (maximum likelihood) and probability threshold crossing (sequential analysis) decision rules, and examine their comparative performance on naturally-generated whisker sensor data.

4 Probabilistic texture discrimination

An initial visual inspection indicates that the data looks like noisy time series with means and variances that vary from texture to texture. All data show dead-zones and jumps where the whisker has either become static (*e.g.* lost contact with the surface) or contacted an irregularity. For the rotating robot motion, there are systematic differences between clockwise and anti-clockwise motion (first and last four trials in Fig. 2) because of the angle of the whisker to the robot body. Meanwhile, the autonomous motion consists of random transitions between these two states, interspersed with a third state of forwards motion. All of these effects present challenges for classifying the textural data, but ones that must be overcome if the classifier is to function robustly for an animal or autonomous robot in a natural environment.

4.1 Training and sampling distributions

The initial 8 seconds of each trial was used for training data, leaving the final 8 seconds of each trial for later validation of the classification algorithms. The data were then pooled under four choices of robot motion: (a) stereotyped anticlockwise motion trials 1-4; (b) stereotyped clockwise motion trials 5-8; (c) either stereotyped motion trials 1-8; and (d) autonomous motion trials 1-4.

The sampling distributions associated with the texture likelihoods of the measured x - and y -sensor voltages were found for the four textures under these four robot motions (Fig. 4). These probabilities were calculated from binning the range of sensor voltages into 10 mV intervals and totaling the number of values in each bin. These totals represented the empirical frequencies of the samples, which when normalized by the sample numbers gave the probability distributions of the sensor values.

The sampling x -distributions (Figs 4a,c,e,g) looked approximately Gaussian, whereas the y -distributions (Figs 4b,d,f,h) were often non-Gaussian with a range of differences across the textures. The y -distributions also tended to be wider than the x -distributions, apparently due to greater vertical motion of the whisker as it bumped along surface features compared with its horizontal motion relative to the robot.

In practice, it was necessary to smooth the sampling distributions to correct for bias in the training data. Without this smoothing, the few samples in the tails of the distributions led to errors in estimating the probabilities, which diminished the performance of the classifier. All sampled

probabilities were thus convolved with a Gaussian smoother of width $\sigma = 100$ mV (10 intervals), which improved classification performance while smoothing on a relatively small scale compared to the overall spread of data.

Figure 4 about here (single column)

4.2 Maximum likelihood classification

Given data from an unknown texture, the sampling distributions plotted in Fig. 4 were first used to construct a texture classifier based on maximum likelihood estimation over fixed temporal window duration [26, 33]. For validation, the data were separated into discrete segments over which the texture was determined. The classifier then identified the maximum of the log likelihood values accumulated over these sampling windows (Eq. 7) as described in Sec. 3.

The proportion of correct classifications, or hits, was calculated for each of the four textures (Figs 5a-d; top row) under the four types of robot motion considered here, namely stereotyped clockwise, anticlockwise and either rotating motion, or autonomous motion under the robot's guidance system. In a previous study [26], using both x - and y -sensor voltage data was found to give the best classification (with no consistency for classification using only single x - or y -sensor data); hence, the present study considered only classification using both sensor directions. Then a feature common across all types of motion and all textures was that the reliability of the classification depended on the window duration, so that as more evidence was used the decision became better. Roughly speaking, the reliability improved greatly as the window duration increased up to about 50-100 ms of data, and then modest gains occurred thereafter.

Comparing the hit rates for the individual stereotyped rotating motions (Figs 5a,b), the maximum likelihood classifier performed accurately over both anticlockwise or clockwise rotating motion. Mean hit rates were 91% and 85% for a 200 ms window. Furthermore, when the classifier was agnostic to the direction of rotation (Fig. 5c), it still performed at similar accuracy, achieving a mean hit rate of 89% over a 200 ms window. Thus, by combining the likelihoods for the clockwise and anticlockwise motion, the classifier was able to perform well on either type of motion, even though the individual likelihoods were very different (*c.f.* Figs 4b and d). This ability to generalize by combining likelihood information was a key aspect of all probabilistic classifiers.

For the autonomous motion (Fig. 5d), the hit rates on two of the four textures (smooth carpet and tarmac) were comparable with the accuracy achieved for stereotyped motion. However, the hit

rates on the two other textures (rough carpet and vinyl) were degraded to about around 60%, which brought the overall mean hit rate on autonomous motion down to 77% for a 200 ms window. Even so, given the considerable complexity of the autonomous motion, consisting of random anticlockwise, clockwise and forward motions, the maximum likelihood classifier demonstrated that it can successfully generalize over these motions by combining the probability distributions.

Figures 5 and 6 about here (double column on same page)

4.3 Sequential Bayes classification

A probabilistic classifier based on Bayesian sequential analysis was then considered. Log posterior probabilities for each of the four textures were evaluated over an increasing duration of test data, with the class given by the maximal value at the time of passing a preset (log) probability threshold (Eq. 8). For validation, the sequential Bayes classifier ran until it made a decision (example shown in Fig. 7), after which the posterior probabilities were reset to their flat prior values of one-quarter and the sequential classification began again. Note that this process is reminiscent of the time course of neuronal activity recorded from the parietal cortex of monkeys during a decision making task (*e.g.* [5, Fig. 5c]).

The hit rates were calculated for each of the four textures under the four types of robot motion (Figs 6a-d; top row) for probability thresholds ranging from 0.5–0.99999999. Similarly to maximum likelihood classification, the accuracy improved with increasing the decision parameter, which here was the probability threshold (whereas maximum likelihood classification varied the decision time directly). For each texture, the decision times had a distribution depending upon the chosen probability threshold (examples in Fig. 8), from which we plotted the mean decision time against the mean hit rate parameterized with the same probability threshold (Figs 6e-h; bottom row). Unlike the maximum likelihood classifier, these timing distributions also depended upon the test texture. For example, vinyl was relatively easy to discriminate and had quick decisions (Fig. 8d), whereas smooth carpet was more difficult and took longer (Fig. 8b). Note that these reaction time distributions are not unlike those found in humans and animals (*e.g.* [6, Fig. 1a]).

The most striking aspect of the hit rates for the sequential Bayes classifier was that they were substantially better than those for the maximum likelihood classifier (*c.f.* Figs 5,6). In particular, mean hit rates over all textures were 6–16% greater than the maximum likelihood method for mean

decision times close to 200 ms. This is consistent because the sequential Bayes classifier chooses the appropriate data duration to classify over (increasing or reducing the sample number with ambiguity or clarity), whereas the maximum likelihood classifier is restricted to a fixed duration.

The overall accuracy of the sequential Bayes classifier was generally as good as could be reasonably expected on noisy data with artifacts such as jumps and dead-zones. For less than 200 ms of data, the average hit rates over all textures were well above 90%, which is considerably better than other classification methods applied to texture data from artificial vibrissa, as discussed later. The classifier was also able to generalize over robot motions by combining likelihood information. For mean decision times ~ 200 ms, there was an overall 95% reliability over both anticlockwise and clockwise rotations. Meanwhile, on autonomous motion the sequential Bayes classifier had a 93% mean hit rate (compared with 77% for the maximum likelihood classifier).

Figure 7 about here (single column)

Figure 8 about here (single column)

5 Comparison with non-probabilistic texture discrimination

Previous studies of texture classification with artificial whisker sensors have utilized the frequency spectrum of the whisker signals [23, 24, 25, 34, 35, 36]. The main idea is that contacts with various textured surfaces will cause whiskers to vibrate at distinct frequencies and amplitudes that are characteristic of the contacted surfaces. Here we consider two methods of classifying the surfaces from their power spectra that have been applied previously to whisker data from mobile robots: spectral template matching [24, 25] and spectral pattern recognition with a neural network [23, 34, 36].

Tables 1-4 about here (two per column, over two columns)

5.1 Spectral template classification

Similarly to Sec. 4.1, training data were taken from the initial 8 seconds of each trial and validation data from the final 8 seconds, with the selection of training and validation data identical for all classifiers considered in this article. The data were separated into 400 ms (800 sample) segments, giving 20 training and 20 validation sets from each of the 12 trials for each of the 4 textures. (Note that this uses at least twice the data of the probabilistic classifiers, but not favoring the spectral methods with less data led to an overly poor resolution of the power spectrum.) These 400 ms segments were then transformed to frequency space by numerical calculation of the discrete fast fourier transform using the Cooley-Tukey algorithm. The power spectrum was then found from the square of the absolute value of the fourier transform value at each frequency (Fig. 9).

Templates for texture classification were constructed from the mean power spectra over these textures in the training data (Fig. 9). These power spectra peaked in the 30-40 Hz range with amplitude characteristic of the texture. Classification was then achieved by calculating the total root-mean-square error from these mean power spectrum templates for each of the four textures, with the least error specifying the chosen class [24, 25]. Discriminators included that tarmac and rough carpet had large surface features (Fig. 1), which led to significant low frequency power for a whisker tip moving at a few cm/sec over cm-scale features. Another discriminator was the amplitude of the resonant peak near 30 Hz, which showed a clear dependence on surface type (Fig. 9), such as from the friction of the whisker tip against the surface.

Results of the spectral template method on validation data were of moderate accuracy, with mean hit rates around 50-70% (Table 3). These hit rates were about 20-40% poorer than the maximum

likelihood classifier and 30-50% poorer than the sequential Bayes classifier.

Figure 9 about here (single column)

5.2 Spectral pattern recognition with neural networks

Another method for classifying texture data from their frequency spectra is to employ pattern recognition techniques via multi-layer neural networks [23, 34, 36]. For proper comparison with the other classifiers, we used the same training and validation data sets employed elsewhere in this article (with 400 ms segments of whisker data sampled at 2 kHz, again favoring these methods over the probabilistic classifiers). The power spectrum was determined similarly to the spectral template method in the previous section. However, to reduce the number of inputs to the neural network only the spectrum up to 120 Hz was considered, since the power above this region is close to zero (Fig. 9)

It is well known that feed-forward neural networks can recognize patterns, for which they are commonly termed multi-layer perceptrons (MLPs). Here we used an MLP with 120 inputs, 20 neurons in the hidden layer and 4 output neurons (one for each texture). Each neuron in the hidden and output layers had a log-sigmoid transfer functions that generated outputs between zero and one. The hidden network weights were learnt using backpropagation and overall optimization achieved via scaled conjugate gradient descent with cost function the root mean square error on the network output. The classification of new test data was then given by the highest output on the MLP outputs, and the hit rates equal to the proportion of correct classification to the overall number of test trials. In the following results, the network was trained 10 times and only used if it converged to a reliable classifier (all hit rates greater than 25%).

Results of the neural network classifier on validation data were of good accuracy, with mean hit rates on all types of motion around 70–80% (Table 4; mean result over 10 training sessions). These hit rates were considerably higher than the spectral template matching method from the previous section. The better performance of the neural network method compared with template matching is not surprising in hindsight, because MLPs are capable of capturing quite complicated relations between data. This does come at a significant expense in computational cost, with the template matching method taking only a fraction of a second to train and the neural network method taking many tens of seconds (on a standard 2 GHz PC with 4 Gb of RAM).

In comparison with the maximum likelihood and sequential Bayes classifiers, the neural network classifier was about 7-17% and 14-24% less accurate respectively.

6 Discussion

Figure 10 about here (single column)

We have shown that a sequential Bayes classifier related to leading proposals for perception in animals out-performs existing alternative accounts of texture discrimination in our physical model of the rat whisker system. In Bayesian sequential analysis, the evidence for competing hypotheses (here percepts of texture) was accumulated over time until reaching a preset threshold when a decision was made. We found that alternative, non-probabilistic classification methods considered previously [25, 24, 34] were generally around 20-50% poorer in accuracy than sequential analysis, while a probabilistic method based on (fixed-response time) maximum likelihood estimation [26, 33] was about 10% poorer.

The better performance of sequential analysis over maximum likelihood estimation originated in using variable reaction times from a probability threshold for decision making. Both of these probabilistic classifiers used an evidence accumulation framework based on log likelihood integration assuming sampling independence over time. The maximum likelihood method was restricted to a predefined decision time, whereas the sequential Bayes classifier dynamically made the decision when at least one inferred posterior probability reached a preset probability threshold. Given that neuronal recordings in monkeys making perceptual decisions suggest a mechanism of probabilistic threshold crossing [3, 4, 5] and that here we have demonstrated clear benefits for texture discrimination with artificial whiskers using a similar decision rule, we suggest that rats may also use this discrimination strategy to perceive texture.

We also found that the performance of the sequential Bayes classifier improved dramatically as the resulting decision times increased up to 100 ms, but improved slowly thereafter. Hence, the optimal integration time in the tradeoff between speed and accuracy would be around 100 ms. It is intriguing that in behaving rats, texture discrimination is achieved over a similar time frame, consisting typically of three to four contacts of about 50 ms duration each [37]. In other words, the rat may collect and analyze three to four samples of whisker vibration in order to make a fast and accurate decision. Thus the time scale is similar in optimizing biological and robot texture classification.

These results inform about sensory encoding in biological systems, specifically rodents, in their relation to various hypotheses about which features of whisker motion are important for texture discrimination. One idea is that the entire set of whiskers functions analogously to the cochlea in

performing frequency analysis [16], due to differences in vibrassae properties across the face [38] resulting in differential resonant frequencies. A related idea is that a single whisker could also use resonance as a texture cue, by considering the variation in oscillation amplitude [35] or mean velocity [13] from the resonant interaction of surface features with the intrinsic whisker dynamics. Another hypothesis stresses instead the kinematic conversion of surface shape into trains of discrete motion events (stick-slips) by individual whiskers [15], such that those with high-velocity (and high-acceleration) can encode textures by their occurrence, number and possibly timing [9, 10, 11, 12, 39, 40]. Meanwhile, another related view is that the mean speed of whisker micro-motion over the contact could also cue for texture [8, 14, 15].

In our robot study of the rat whisker system, the artificial whisker resonated when contacting natural surfaces, as was evident from both the fine detail of the whisker contact (Fig. 10) and the peak near 30 Hz in the frequency spectra (Fig. 9). The amplitude of this oscillation varied systematically with surface roughness to give a discriminator for the probabilistic classifiers from the variance of the sampling distributions associated with each likelihood (Fig. 4). Therefore in the present robot study the probabilistic classifiers utilized changes in resonance amplitude to discriminate texture. However, recent experimental evidence found that the power spectra of rat whisker movements during voluntary palpation of various sandpaper surfaces have little systematic variation with texture [10, Figs 7c,d]. Taken on face value, this result suggests that the rat does not extract the same kinematic features as the robot with a biomimetic whisker and probabilistic classifier over the time series of whisker deflections.

Closer examination does however reveal some subtleties when directly comparing biological studies with the present robot treatment, which are informative about both how the biological system is configured for tactile sensing and how robots could better utilize artificial whisker sensors.

An argument against the resonance hypothesis was that the power of the whisker vibrations at the resonance frequency does not vary substantially across textures, and therefore can not discriminate surfaces [10]. However, a visual inspection of the power spectra from the biomimetic whisker in the present study (Fig. 9) revealed only a small amount of systematic variation between several textures, and yet the surfaces can be reliably identified to about 70-80% with a neural network classifier of the power spectrum (Table 4). Therefore what may appear to be small differences in the overall shape of the power spectra can be sufficient for reasonable classification. In our view, the most convincing way to demonstrate that the power spectra are not sufficient for reliable classification is to apply

an appropriate classifier to the whisker signals, such as the neural network method considered here, which was not attempted in the original study [10].

Furthermore, the probabilistic classifiers (sequential analysis and maximum likelihood) must also use features other than the resonance amplitude to achieve better performance than classifiers based solely on the power spectra. A distinctive feature is that mean whisker positional deflection (evident in Fig. 4) varied systematically with surface roughness, as was also evident in the whisker deflection profiles (Fig. 10). Physically, as the friction between the surfaces and the whisker increased, the whisker was dragged back more strongly, which led to greater mean deflection. This signal component is not usually considered in the biological literature, even though the animal has information about whisker position at the thalamic relay to sensory cortex [41]. The contribution of this effect to the perception of texture could be investigated in behavioral experiments, for example by checking whether rodents can discriminate surfaces of equal roughness but differing friction or by presenting de-measured artificial whisker vibrations.

In general, discrimination based on the probabilistic classifiers will use all the available evidence in the likelihood function to give the best decision. In the present robot experiment with fixed, passive biomimetic whiskers, this evidence related to the amplitude of the whisker resonance and its mean deflection, as represented in the mean and variance of the sampling distributions associated with the likelihoods. However, in rodent experiments such as those described above [10, 11, 40], the whiskers were actively dabbed against surfaces rather than passively brushed along them; moreover, the scale of the whiskers was such that the resonance shifted to higher frequencies (around 100 Hz rather than 30 Hz). In such circumstances, it appears from the biology that stick-slip events overtake the resonance amplitude as the dominant signal component for reliable texture discrimination [9, 10, 11, 12, 39, 40].

To investigate these proposals further in a robot implementation would require a follow-up study in which the whiskers are actuated rather than mounted in a fixed position, such as with the BIOTACT sensor which consists of a whisking head mounted on a robot arm [28]. The head of the BIOTACT sensor has multiple whiskers of differing lengths akin to rodent vibrissae, also allowing investigation of multi-whisker integration and the effect of whisker dynamics on discrimination. (For example, shortening whiskers to reduce interference between the resonance and micro-features of the surface has been reported to improve texture discrimination [23].) Direct control of the head and whiskers would also allow study of reaction-time and perception in an artificial device, for example

by manipulating the costs of making errors and delaying decisions, which are fundamental aspects of animal perception [5].

The value of this approach for understanding biological sensing is that the experimenter can design the robot to test theories motivated by the biology, whereas biology is principally an empirical science based on systems that are given. Combining both biological and engineering approaches, through biomimetics, can in principle answer questions that are not answerable by biology alone [42]. The results presented here cast light on how the various previous proposals for rodent texture discrimination are dependent on the whisker contact mechanics, and suggest a number of potential lines of enquiry for future neurobiological studies. We would also anticipate that extending our biomimetic approach to robotic systems that incorporate additional aspects of biological vibrissal sensing, such as active control of whisker movement, should help resolve these issues in tactile sensing and contribute to a common account of decision making across mammalian species

Acknowledgment

The authors thank members of ATLAS (Active Touch Laboratory At Sheffield), the Bristol Robotics Laboratory, the BIOTACT (BIOMimetic Technology for vibrissal ACtive Touch) consortium and the anonymous reviewers. This work was supported by EU Framework project BIOTACT (ICT-215910), by the Human Frontier Science Program (contract RG0041/2009-C), the Compagnia San Paolo, and the Italian Institute of Technology through the BMI Project.

References

- [1] D.C. Knill and A. Pouget. The Bayesian brain: the role of uncertainty in neural coding and computation. *TRENDS in Neurosciences*, 27(12):712–719, 2004.
- [2] D. Kersten, P. Mamassian, and A. Yuille. Object perception as Bayesian inference. *Annu. Rev. Psychol.*, 55:271–304, 2004.
- [3] A.C. Huk and M.N. Shadlen. Neural activity in macaque parietal cortex reflects temporal integration of visual motion signals during perceptual decision making. *Journal of Neuroscience*, 25(45):10420, 2005.
- [4] M.L. Platt and P.W. Glimcher. Neural correlates of decision variables in parietal cortex. *Nature*, 400(6741):233–238, 1999.
- [5] J.I. Gold and M.N. Shadlen. The neural basis of decision making. *Annu. Rev. Neurosci.*, 30:535–574, 2007.
- [6] R. Bogacz, E. Brown, J. Moehlis, P. Holmes, and J.D. Cohen. The physics of optimal decision making: A formal analysis of models of performance in two-alternative forced-choice tasks. *Psychological Review*, 113(4):700, 2006.
- [7] A. Wald and J. Wolfowitz. Optimum character of the sequential probability ratio test. *The Annals of Mathematical Statistics*, 19(3):326–339, 1948.
- [8] T. Morita, H. Kang, J. Wolfe, S.P. Jadhav, and D.E. Feldman. Psychometric curve and behavioral strategies for whisker-based texture discrimination in rats. *PloS one*, 6(6):e20437, 2011.
- [9] M.E. Diamond. Texture sensation through the fingertips and the whiskers. *Current opinion in neurobiology*, 20(3):319–327, 2010.
- [10] J. Wolfe, D.N. Hill, S. Pahlavan, P.J. Drew, D. Kleinfeld, and D.E. Feldman. Texture coding in the rat whisker system: slip-stick versus differential resonance. *PLoS Biol*, 6(8):e215, 2008.
- [11] M.E. Diamond, M. Von Heimendahl, and E. Arabzadeh. Whisker-mediated texture discrimination. *PLoS Biol*, 6(8):e220, 2008.

- [12] M.E. Diamond, M. von Heimendahl, P.M. Knutsen, D. Kleinfeld, and E. Ahissar. ‘Where’ and ‘what’ in the whisker sensorimotor system. *Nature Reviews Neuroscience*, 9(8):601–612, 2008.
- [13] J.T. Ritt, M.L. Andermann, and C.I. Moore. Embodied information processing: vibrissa mechanics and texture features shape micromotions in actively sensing rats. *Neuron*, 57(4):599–613, 2008.
- [14] M. Von Heimendahl, P.M. Itskov, E. Arabzadeh, and M.E. Diamond. Neuronal activity in rat barrel cortex underlying texture discrimination. *PLoS biology*, 5(11):e305, 2007.
- [15] E. Arabzadeh, E. Zorzin, and M.E. Diamond. Neuronal encoding of texture in the whisker sensory pathway. *PLoS Biology*, 3(1):e17, 2005.
- [16] M.A. Neimark, M.L. Andermann, J.J. Hopfield, and C.I. Moore. Vibrissa resonance as a transduction mechanism for tactile encoding. *The Journal of neuroscience*, 23(16):6499, 2003.
- [17] T.J. Prescott, M.J. Pearson, B. Mitchinson, J.C.W. Sullivan, and A.G. Pipe. Whisking with robots from rat vibrissae to biomimetic technology for active touch. *IEEE Robotics and Automation Magazine*, 16(3):42–50, 2009.
- [18] J.H. Solomon and M.J.Z. Hartmann. Artificial whiskers suitable for array implementation: Accounting for lateral slip and surface friction. *IEEE Transactions on Robotics*, 24(5):1157–1167, 2008.
- [19] D.E. Kim and R. Moller. Biomimetic whiskers for shape recognition. *Robotics and Autonomous Systems*, 55(3):229–243, 2007.
- [20] J.H. Solomon and M.J. Hartmann. Biomechanics: Robotic whiskers used to sense features. *Nature*, 443(7111):525, 2006.
- [21] M.J. Pearson, I. Gilhespy, C. Melhuish, B. Mitchinson, M. Nibouche, A.G. Pipe, and T.J. Prescott. A biomimetic haptic sensor. *International Journal of Advanced Robotic Systems*, 2(4):335–343, 2005.
- [22] A.E. Schultz, J.H. Solomon, M.A. Peshkin, and M.J. Hartmann. Multifunctional whisker arrays for distance detection, terrain mapping, and object feature extraction. *Proc. IEEE Int. Conf. Robot. Autom. (ICRA 2005)*, pages 2588–2593, 2005.

- [23] D.E. Kim and R. Moeller. A biomimetic whisker for texture discrimination and distance estimation. In *From Animals to Animats 8*, page 140. The MIT Press, 2004.
- [24] M. Fend, S. Bovet, H. Yokoi, and R. Pfeifer. An active artificial whisker array for texture discrimination. In *Proc. IEEE Int. Conf. Intelligent Robots and Systems (IROS 2003)*, volume 2, pages 1044–1049, 2003.
- [25] M. Evans, C.W. Fox, M.J. Pearson, and T.J. Prescott. Spectral template based classification of robotic whisker sensor signals in a floor texture discrimination task. *Proceedings of Towards Autonomous Robotic Systems (TAROS 2009)*, pages 19–24, 2009.
- [26] N.F. Lepora, M. Evans, C.W. Fox, M.E. Diamond, K. Gurney, and T.J. Prescott. Naive bayes texture classification applied to whisker data from a moving robot. In *The IEEE 2010 International Joint Conference on Neural Networks (IJCNN)*, pages 1–8, 2010.
- [27] M.J. Pearson, B. Mitchinson, J.C. Sullivan, A.G. Pipe, and T.J. Prescott. Biomimetic vibrissal sensing for robots. *Philosophical Transactions of the Royal Society B: Biological Sciences*, 366(1581):3085–3096, 2011.
- [28] J. Sullivan, B. Mitchinson, M. Pearson, M. Evans, N. Lepora, C. Fox, C. Melhuish, and T. Prescott. Tactile discrimination using active whisker sensors. *IEEE Sensors*, 2011.
- [29] B. Mitchinson, T.S. Chan, J. Chambers, M. Pearson, M. Humphries, C. Fox, K. Gurney, and T.J. Prescott. BRAHMS: Novel middleware for integrated systems computation. *Advanced Engineering Informatics*, 24(1):49–61, 2010.
- [30] J.I. Gold and M.N. Shadlen. Neural computations that underlie decisions about sensory stimuli. *Trends in Cognitive Sciences*, 5(1):10–16, 2001.
- [31] J.M. Wooldridge. *Introductory econometrics: A modern approach*. South-Western Pub, 2009.
- [32] VP Dragalin, A.G. Tartakovsky, and V.V. Veeravalli. Multihypothesis sequential probability ratio tests. I. Asymptotic optimality. *Information Theory, IEEE Transactions on*, 45(7):2448–2461, 1999.
- [33] N.F. Lepora, C. Fox, M. Evans, B. Mitchinson, A. Motiwala, J.C. Sullivan, M. Pearson, J. Welsby, T. Pipe, K. Gurney, and T. Prescott. A general classifier of whisker data using

- stationary naive Bayes: application to BIOTACT robots. In *Towards Autonomous Robotic Systems*, Lecture Notes in Computer Science.
- [34] M. Fend. Whisker-based texture discrimination on a mobile robot. *Advances in Artificial Life*, pages 302–311, 2005.
- [35] J. Hipp, E. Arabzadeh, E. Zorzin, J. Conradt, C. Kayser, M.E. Diamond, and P. Konig. Texture signals in whisker vibrations. *Journal of neurophysiology*, 95(3):1792, 2006.
- [36] C.W. Fox, B. Mitchinson, M.J. Pearson, A.G. Pipe, and T.J. Prescott. Contact type dependency of texture classification in a whiskered mobile robot. *Autonomous Robots*, 26(4):223–239, 2009.
- [37] Y. Zuo, I. Perkon, and M.E. Diamond. Whisking and whisker kinematics during a texture classification task. *Philosophical Transactions of the Royal Society B: Biological Sciences*, 366(1581):3058–3069, 2011.
- [38] M. Brecht, B. Preilowski, and M.M. Merzenich. Functional architecture of the mystacial vibrissae. *Behavioural brain research*, 84(1-2):81–97, 1997.
- [39] E. Lottem and R. Azouz. Dynamic translation of surface coarseness into whisker vibrations. *Journal of neurophysiology*, 100(5):2852, 2008.
- [40] S.P. Jadhav, J. Wolfe, and D.E. Feldman. Sparse temporal coding of elementary tactile features during active whisker sensation. *Nature Neuroscience*, 12(6):792–800, 2009.
- [41] R.S. Petersen, M. Brambilla, M.R. Bale, A. Alenda, S. Panzeri, M.A. Montemurro, and M. Maravall. Diverse and temporally precise kinetic feature selectivity in the VPM thalamic nucleus. *Neuron*, 60(5):890–903, 2008.
- [42] B. Mitchinson, M. Pearson, T. Pipe, and T.J. Prescott. In biomimetic robots as scientific models: a view from the whisker tip. *Neuromorphic and Brain-Based Robots*, page 23, 2011.

Table 1: Maximum likelihood classifier

200 ms temporal window (400 samples)

Robot motion	Rough carpet	Smooth carpet	Tarmac	Vinyl flooring	Mean hit rate
anticlockwise	80%	94%	91%	100%	91%
clockwise	74%	84%	84%	97%	85%
rotating	82%	87%	88%	99%	89%
autonomous	57%	90%	93%	68%	77%

Table 2: Sequential Bayes classifier

Decisions taking close to 200 ms (400 samples)

Robot motion	Rough carpet	Smooth carpet	Tarmac	Vinyl flooring	Mean hit rate
anticlockwise	99%	98%	99%	100%	99%
clockwise	91%	84%	94%	98%	92%
rotating	96%	89%	97%	99%	95%
autonomous	85%	97%	99%	91%	93%

Table 3: Template classifier of power spectrum

Fourier transform over 400 ms window (800 samples)

Robot motion	Rough carpet	Smooth carpet	Tarmac	Vinyl flooring	Mean hit rate
anticlockwise	65%	64%	54%	100%	71%
clockwise	36%	53%	3%	96%	47%
rotating	32%	60%	49%	97%	48%
autonomous	6%	43%	83%	79%	53%

Table 4: Neural network classifier of power spectrum

Fourier transform over 400 ms window (800 samples)

Robot motion	Rough carpet	Smooth carpet	Tarmac	Vinyl flooring	Mean hit rate
anticlockwise	68%	84%	84%	99%	84%
clockwise	48%	56%	72%	94%	68%
rotating	68%	81%	79%	97%	81%
autonomous	62%	57%	91%	96%	76%

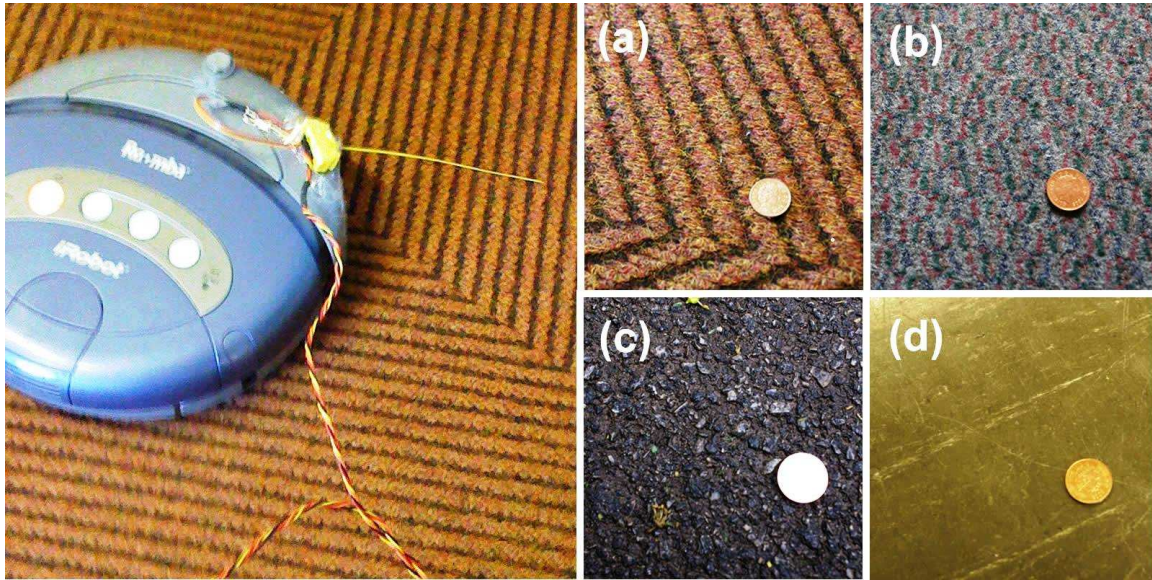


Figure 1: The robot with whisker attachment (online version in color).

A Roomba robot was used as a platform for the experiments. The whisker was mounted on the front of the robot, angled down to make constant contact with the floor. The panels show the various textured surfaces: (a) rough carpet; (b) smooth carpet; (c) tarmac and (d) vinyl.

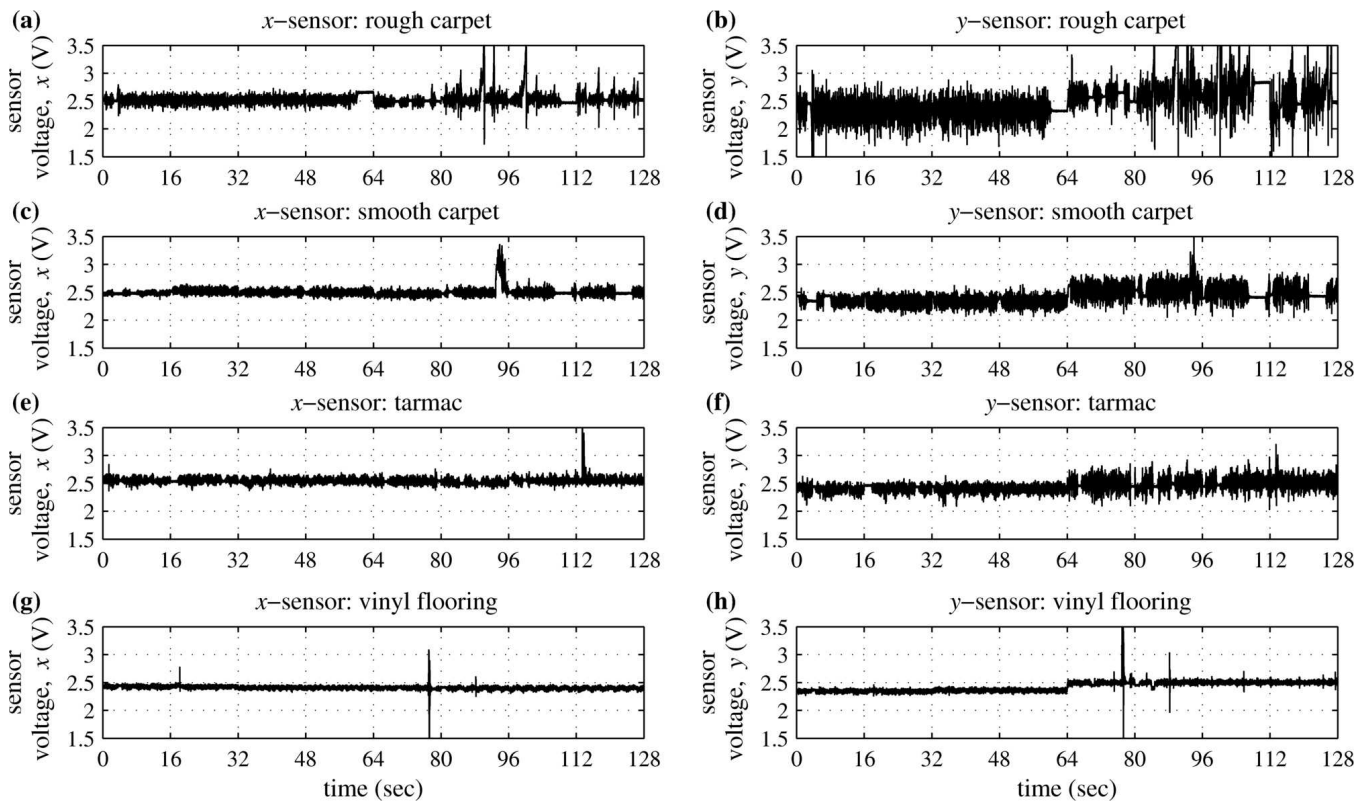


Figure 2: Stereotyped motion data.

Data for the four floor surface textures were collected in eight trials each of length sixteen seconds. The first four trials were for anticlockwise rotating motion and the last four trials were for clockwise motion.

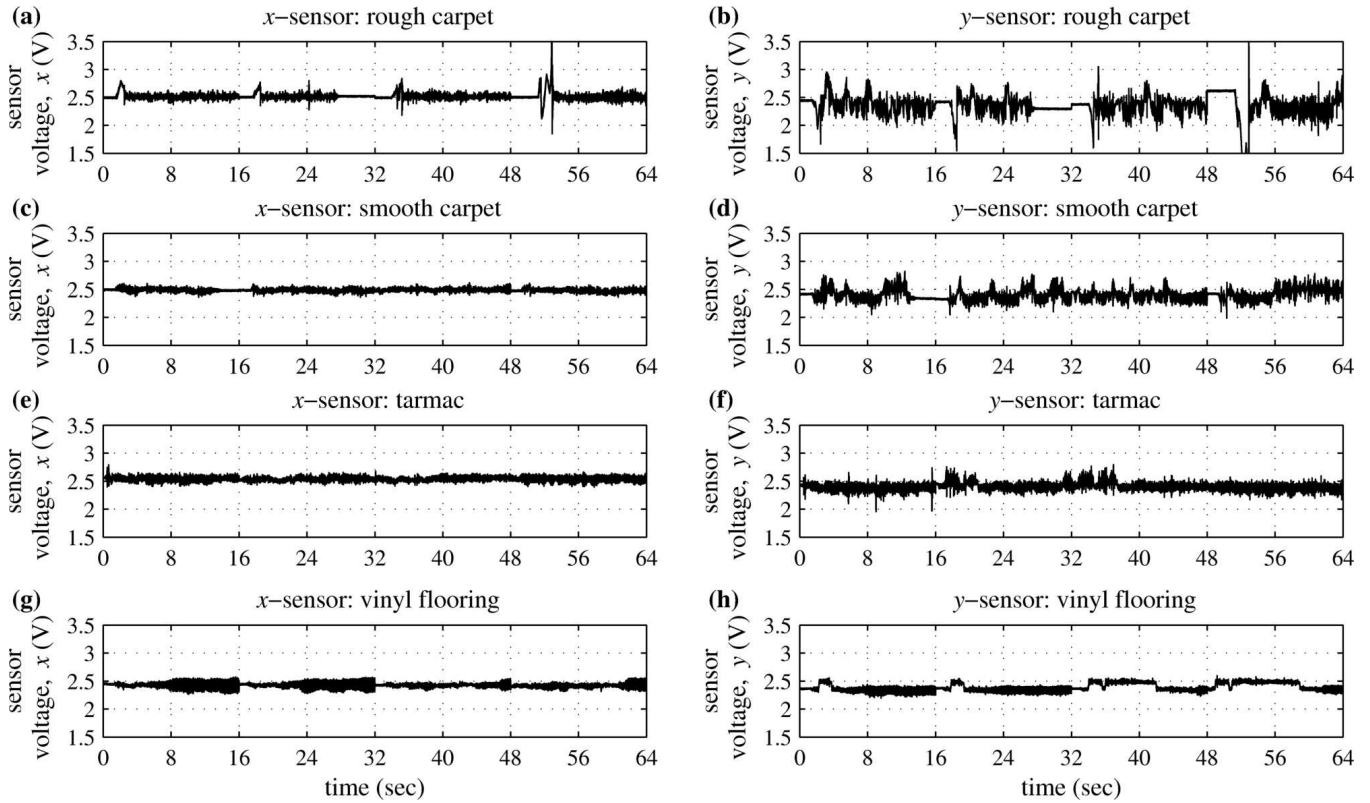


Figure 3: Autonomous motion data.

Data collection as for Fig. 2, but with the robot moving autonomously in a series of externally unpredictable anticlockwise, clockwise and forward motions.

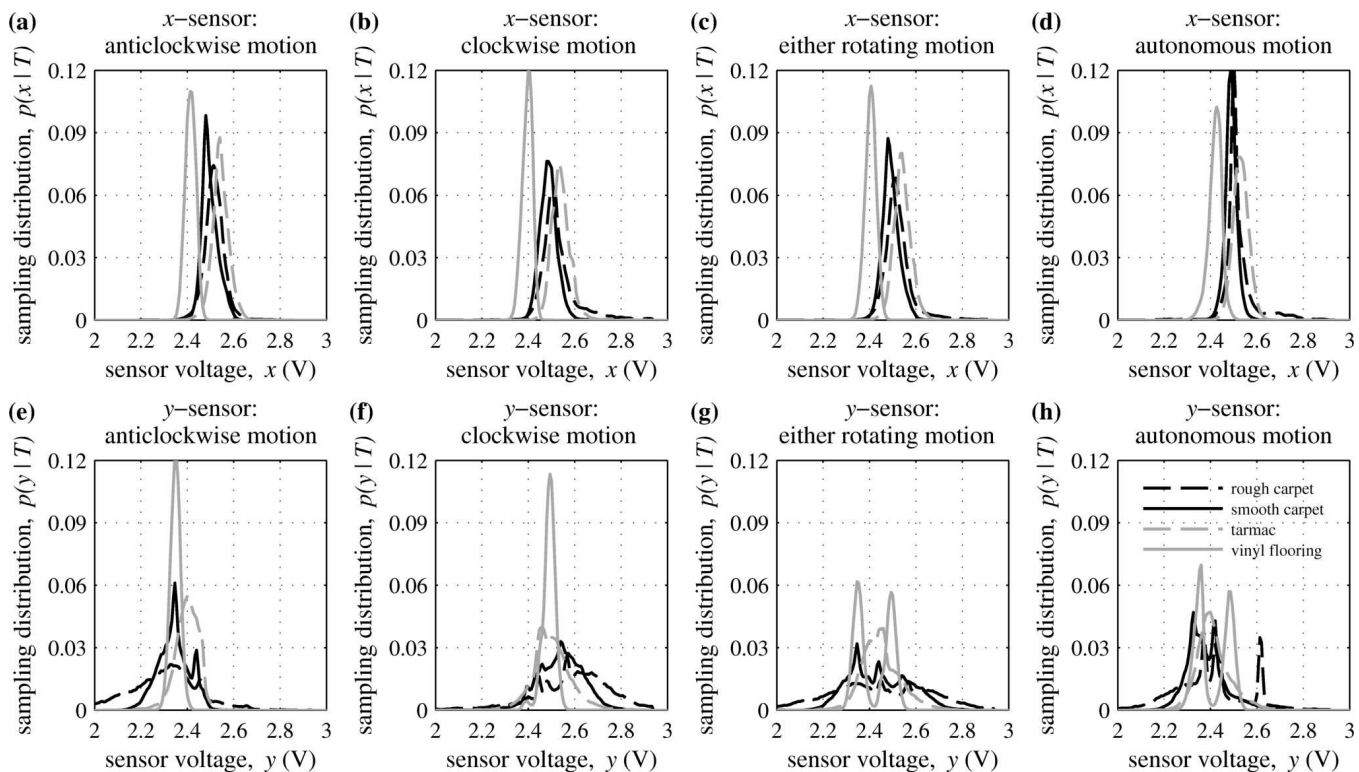


Figure 4: Texture sampling distributions.

The sampling distributions associated with texture likelihoods were calculated from the empirical frequencies with which the samples occurred in training data for the four textures. The top panels show the distributions from the sensor x -component and the bottom panels show the y -component. The horizontal groups of panels are ordered by robot motion, for anticlockwise, clockwise, either rotating and autonomous motion.

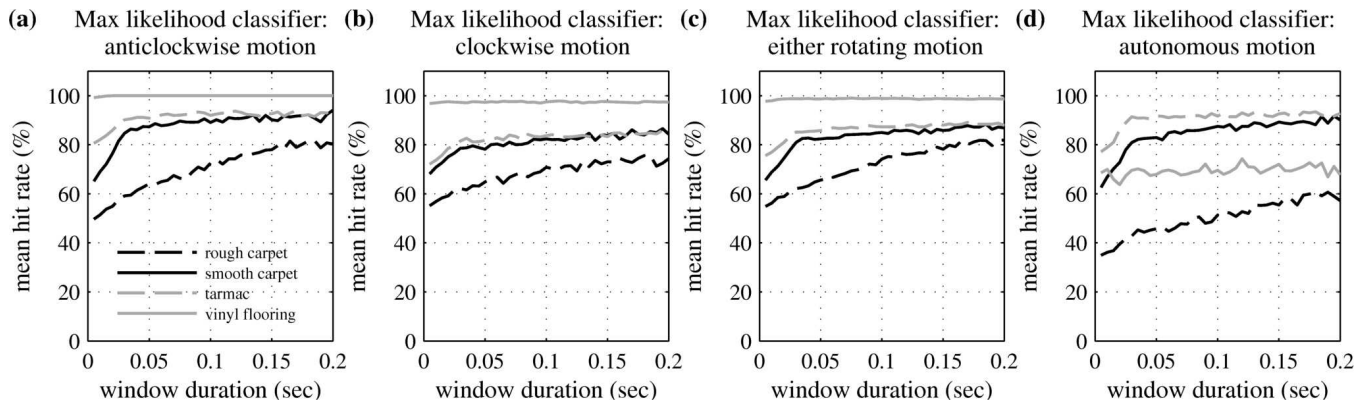


Figure 5: Hit rates for maximum likelihood classifier.

The percentages of correct classification were evaluated over validation data from the four textures for the maximum likelihood classifier with fixed window durations. The four types of robot motion (stereotyped anticlockwise, clockwise, either rotation and autonomous motion) were considered separately.

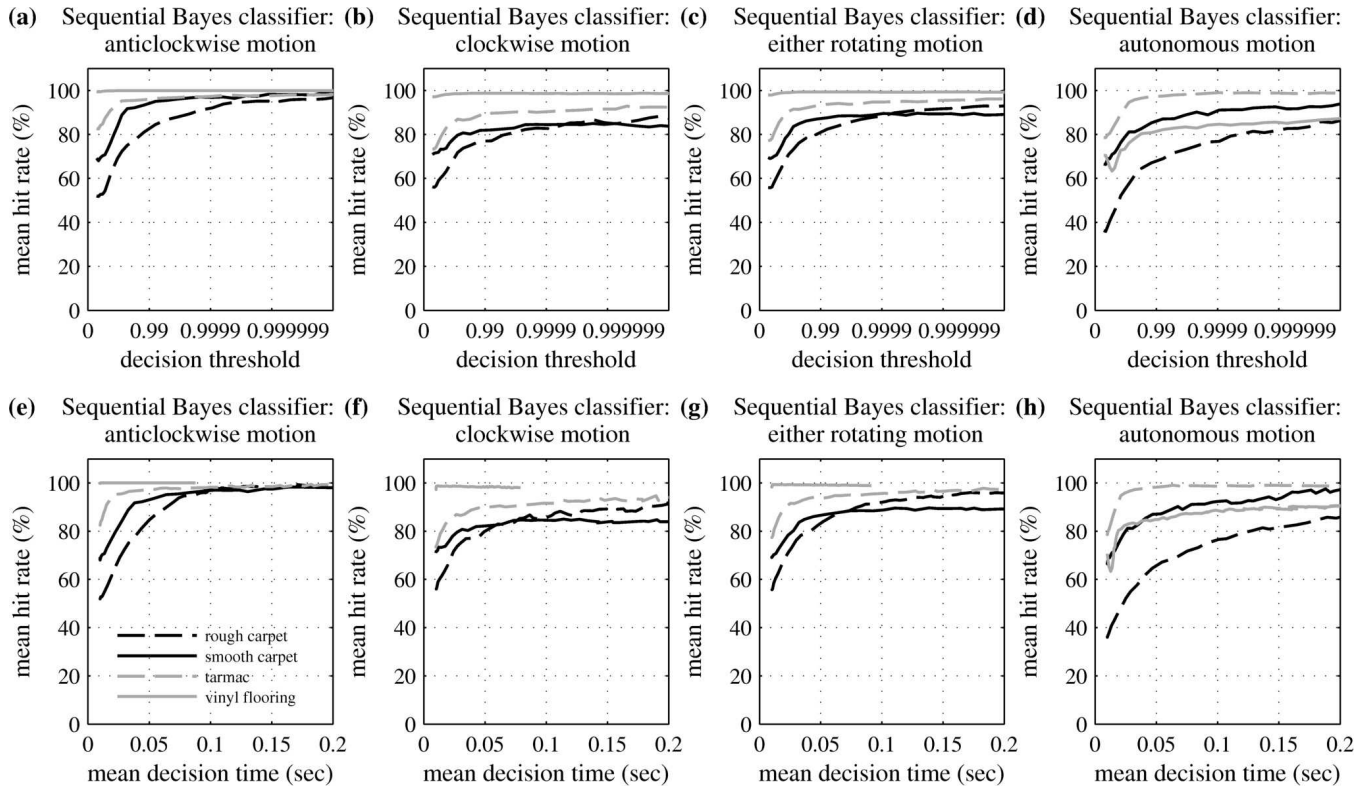


Figure 6: Hit rates for sequential Bayes classifier.

The percentages of correct classification were evaluated over validation data from the four textures for the sequential Bayes classifier. The four types of robot motion (stereotyped anticlockwise, clockwise, either rotation and autonomous motion) were considered separately. The top row (panels a-d) displays the mean hit rate plotted against decision threshold and the bottom row (panels e-h) plots this mean hit rate against the mean decision time calculated at the same decision threshold.

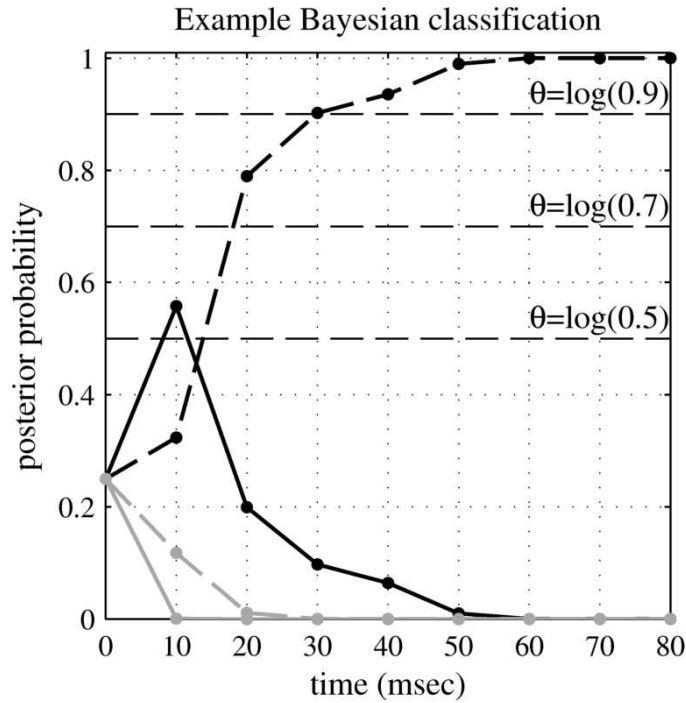


Figure 7: Example texture discrimination for the sequential Bayes classifier.

The posterior probabilities are plotted against increasing the window duration of sampled test data (for rough carpet; texture classes denoted with the line styles from Figs 4-6). Probability thresholds of 0.5, 0.7 and 0.9 are also shown, giving decision times of 10 ms, 20 ms and 30 ms respectively.

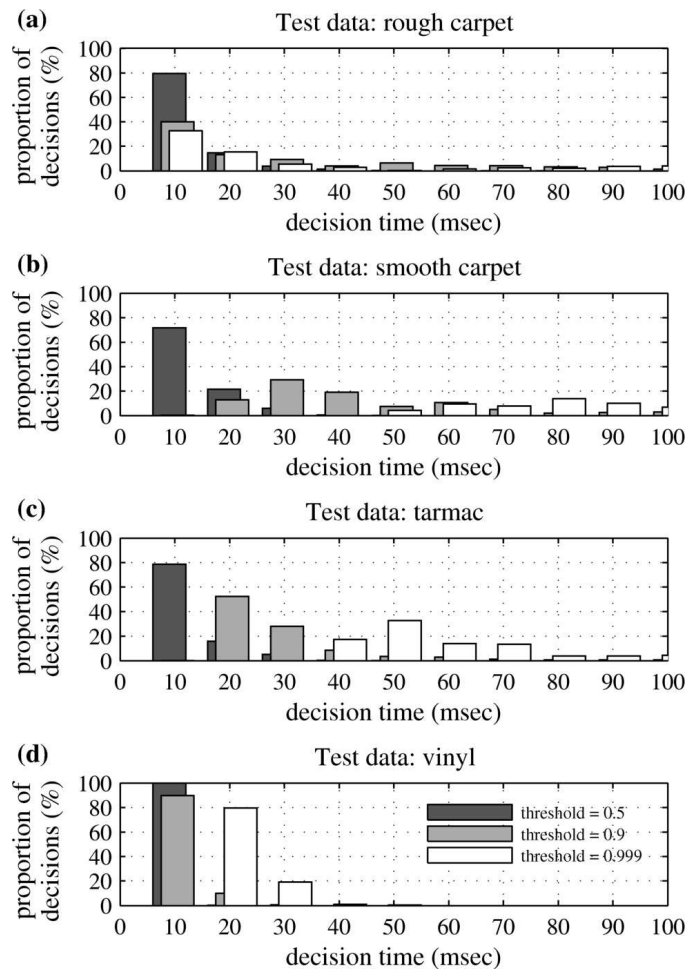


Figure 8: Example decision times for the sequential Bayes classifier.

Histograms of the decision times are shown for each of the four textures. Data were taken from the stereotyped rotating motion, with probability thresholds 0.5, 0.9 and 0.999.

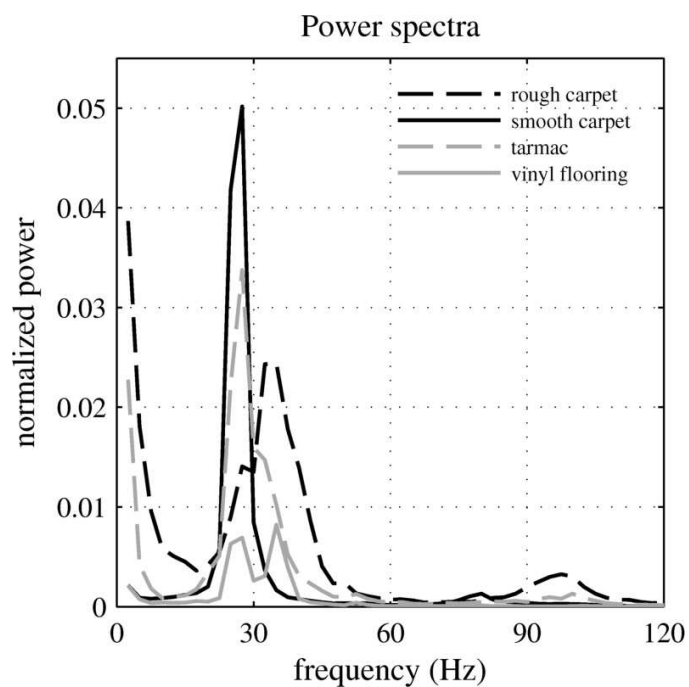


Figure 9: Power spectra of whisker signals.

Whisker deflection power spectra are shown for trials 1 to 4 (anticlockwise rotating motion), which were taken over 400 ms windows and then averaged. These spectra are normalized by the mean total power for all textures.

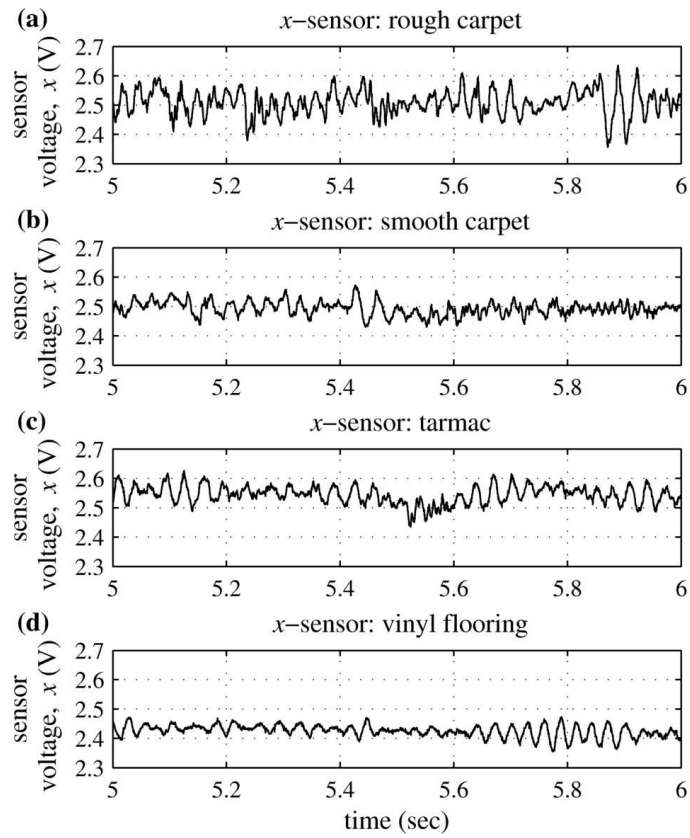


Figure 10: Whisker deflection profiles for four textures.

Whisker deflection profiles are shown for trial 1 (from 5 to 6 seconds).